The Eurasia Proceedings of Science, Technology, Engineering & Mathematics (EPSTEM)
ISSN: 2602-3199

The Eurasia Proceedings of Science, Technology, Engineering & Mathematics (EPSTEM), 2024

Volume 31, Pages 64-72

ICATI 2024: International Conference on Advances in Technology and Innovation

Comparative Analysis of the Flight Characteristics and Energy Efficiency of a Quadcopter and an Octacopter

Martin Milenov Kambushev
Georgi Benkovski Bulgarian Air Force Academy

Kiril Milenov Kambushev
Georgi Benkovski Bulgarian Air Force Academy

Abstract: This publication is part of a study aimed at finding the optimal configuration (tricopter, quadcopter, octacopter, etc.) in terms of flight stability, payload and energy efficiency. For this purpose, full non-linear quadcopter and octacopter models have been created. Data from real objects (linear and weight characteristics, parameters of the engine-propeller system) were used to create them. Quadcopter and Octacopter use the same motors and propellers. In the simulations, the mass of the two objects is the same. Both models are controlled with PID controllers in four channels (Yaw, pitch, roll and height). The initial adjustment of the regulators was carried out according to the second method of Ziegler-Nichols. A secondary adjustment of the regulators was carried out, with the goal of minimal over-adjustment, speed and accuracy. A parallel simulation of the nonlinear models in the Simulink environment was performed, on the basis of which the conclusions about the stability and energy efficiency of the quadcopter and the octacopter were made.

Keywords: Quadcopter, Octacopter, Energy efficiency, Sustainability, PID controller

Introduction

At the beginning of the twentieth century, a number of models of human-controlled quadcopters appeared. These vehicles are one of the first that can successfully be used for vertical take-off and landing. However, early prototypes performed poorly and later ones were difficult to steer due to their instability and limited control capabilities. The Breguet brothers' Gyroplane No.I was one of the earliest attempts to create a propeller-driven aircraft (Figure 1.) On September 29, 1907, Gyroplane No.I flew for the first time, albeit at altitude only 0.6 meters. It was neither controllable nor maneuverable, but it was the first time a rotorcraft lifted itself and a pilot into the air. Later the apparatus rose to a height of 1.52 m above the ground (Aviastar.org, n.d.).

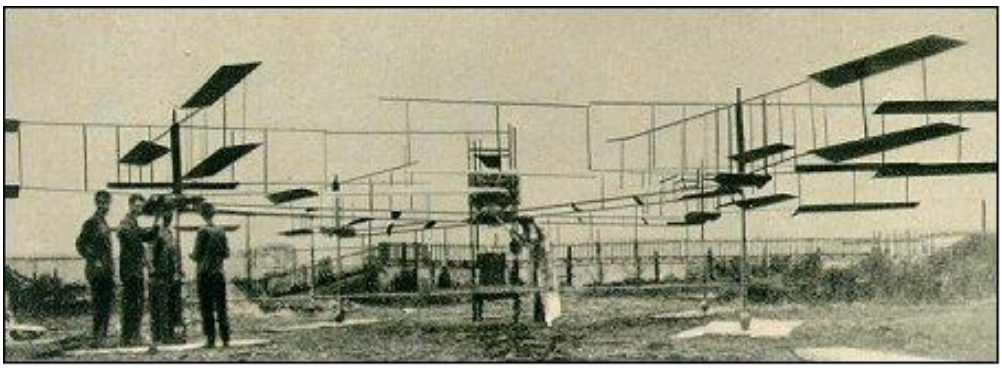

Figure 1. Breguet brothers gyroplane No.I - 1907

In recent years, the development of unmanned aerial vehicles has been very rapid. They are widely used in the civil and military spheres. Civilian applications of UAVs range from transportation and media to agriculture and construction. The wars in Ukraine and the Middle East show in practice the diverse application of unmanned aerial vehicles in real combat operations. Their use has become a must-have element for achieving success on the battlefield. Their widespread use does not mean that UAVs are ideal. They are in a stage of rapid development, especially in relation to the stability and safety of the flight (Biliderov, 2024), its duration and energy efficiency (Georgiev, 2022). This post is part of a study that will compare the features of different types of copters. This is a study on the properties of a quadcopter and an octacopter with the same engines, propellers, and weight. The aim of the research is to determine the optimal configuration in terms of sustainability and energy efficiency.

Mathematical Models

A quadcopter and an octacopter differ in the number of motors, their placement, and the controls required. To make it possible to compare the characteristics of the two models, the same engines, propellers and batteries were used in their creation. The mass of both devices is the same 1.5 kg. This corresponds to a class 450 copter type UAV.

Non-linear mathematical models of quadcopter and octacopter have been created. The two models consist of 12 nonlinear differential equations each. The motion of the center of mass of an unmanned aerial vehicle in an inertial coordinate system is described by the vector equation of Newton's second law:

$$m\frac{d\vec{V}}{dt} = \sum \vec{F} \tag{1}$$

After equation (1) is developed along the axes of the coupled coordinate system, the complete differential equations for the translational motion of the center of mass are obtained:

$$\begin{aligned} \dot{V}_x &= \frac{dV_x}{dt} = \frac{F_x}{m} - \omega_y V_z + \omega_z V_y \\ \dot{V}_y &= \frac{dV_y}{dt} = \frac{F_y}{m} - \omega_z V_x + \omega_x V_z \\ \dot{V}_z &= \frac{dV_z}{dt} = \frac{F_z}{m} - \omega_x V_y + \omega_y V_x \end{aligned} \tag{2}$$

The kinetic momentum change theorem is used to describe the rotational motion around the axes of the connected coordinate system.

$$\frac{d\vec{K}}{dt} = \sum \vec{M} \tag{3}$$

The complete equations for the rotational motion around the center of mass are:

$$\begin{aligned} \dot{\omega}_x &= \frac{1}{I_x}\left[M_x - \left(I_z - I_y\right)\omega_y\omega_z\right]; \\ \dot{\omega}_y &= \frac{1}{I_y}\left[M_y - (I_x - I_z)\omega_z\omega_x\right] \\ \dot{\omega}_z &= \frac{1}{I_z}\left[M_z - \left(I_y - I_x\right)\omega_x\omega_y\right] \end{aligned} \tag{4}$$

Quadcopter and Octacopter are symmetrical aircraft. The lifting force in them is created respectively by two pairs of engines, in the case of the quadcopter, and four pairs of engines, in the case of the octacopter. The propellers rotate (in pairs) in opposite directions as shown in Fig.1 and Fig.2. They don't have the problem with the reactive moment created by the rotating propellers. Before deriving the expressions for the forces and moments acting on the aircraft, the following assumptions must be made:

- Quadcopter and Octacopter are treated as an absolute rigid body, which means that the distance between two arbitrarily chosen points of it remains constant during the flight;
- The mass of the aircraft does not change during flight;
- The mass of the aircraft is symmetrically distributed. From this assumption it follows that the cross moments of inertia $I_{zx} = I_{xz} = I_{yz} = I_{zy} = I_{xy} = I_{yx} = 0$.

After the assumptions made, the motion of each of the two apparatuses can be described as the motion of an absolutely rigid body with six degrees of freedom. For reliable modeling of the movement of aircraft, it is necessary to take into account the dynamics of changes in the lift force and the reactive moment created by each engine. The lift force and the reactive moment are calculated using formula 5. The angular velocity of the rotor i, denoted ω_i creates an axial force f_i. The angular velocity and acceleration of the rotor also create a reactive moment around the rotor axis.

$$\begin{aligned} f_i &= k\omega_i^2, \\ \tau_{M_i} &= b\omega_i^2 + I_M\dot{\omega}_i, \end{aligned} \tag{5}$$

Where: k is a constant proportional to the thrust. It depends on the geometric characteristics of the propeller;
b is a constant proportional to the reactive moment;

- I_M the moment of inertia of the rotor.

In the mathematical modeling of the aircraft and the simulations, the following right-oriented rectangular coordinate systems were used:

- Earth or starting coordinate system Figure 2. Its origin M_1 is fixed on the earth's surface. It is the departure point or the first point of a partially orthodromic route. The M_1Zg axis is directed up the local vertical, and the direction of the other two axes is chosen according to the task so that they form a right-oriented rectangular coordinate system. Normally, the M_1Xg axis is directed in the direction of the runway for airplane-type aircraft (actually the direction of the first partial orthodrome) or in the north direction for copter-type aircraft
- The origin O of the body-fixed coordinate system is located at its center of mass fig. 3 and fig. 4. Axes OX, OY and OZ are rigidly connected to the aircraft, coincide with the main inertial axes and set its position in space.

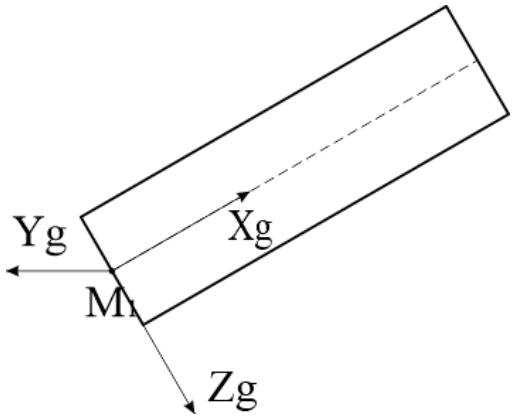

Figure 2. Starting coordinate system

Mathematical Model of a Quadcopter

The mathematical model of a quadcopter is created based on expressions (2) and (4). In equations (2) F_x F_y F_z denote the external forces acting on the aircraft. They are described in more detail with the following expressions:

$$\begin{bmatrix} F_x \\ F_y \\ F_z \end{bmatrix} = \begin{bmatrix} -G.sin(\vartheta) \\ f_1 + f_2 + f_3 + f_4 - G.cos(\gamma)cos(\vartheta) \\ G.sin(\gamma)cos(\vartheta) \end{bmatrix}, \tag{6}$$

where: G – force of gravity directed along the local vertical;
f_1, f_2, f_3, f_4 - forces created by the four engines;

γ, ϑ – bank and pitch angles. Determine the mutual position between the Earth and the body-fixed frame.

Substituting (6) into (2) yields the first three differential equations (7) of the mathematical model.

$$\begin{bmatrix}\dot{V}_x\\ \dot{V}_y\\ \dot{V}_z\end{bmatrix}=\frac{1}{m}\begin{bmatrix}-G.sin(\vartheta)\\ f_1+f_2+f_3+f_4-G.cos(\gamma)cos(\vartheta)\\ G.sin(\gamma)cos(\vartheta)\end{bmatrix}-\begin{bmatrix}0 & -\omega_z & \omega_y\\ \omega_z & 0 & -\omega_x\\ -\omega_y & \omega_x & 0\end{bmatrix}\times\begin{bmatrix}V_x\\ V_y\\ V_z\end{bmatrix} \quad (7)$$

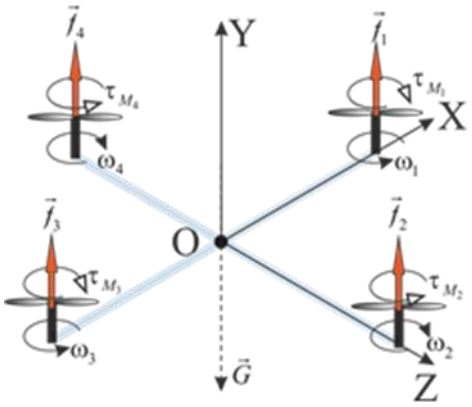

Figure 3. The distribution of external forces and moments acting on a quadcopter

The rotation around the center of mass is described by expressions (4). In them $\begin{matrix}M_x\\ M_y\\ M_z\end{matrix}$ are the external moments acting along the axes of the connected coordinate system of the copter. They are described in more detail with the following expressions:

$$\begin{bmatrix}M_x\\ M_y\\ M_z\end{bmatrix}=\begin{bmatrix}h(f_4-f_2)\\ \tau_{M_1}-\tau_{M_2}+\tau_{M_3}-\tau_{M_4}\\ h(f_1-f_3)\end{bmatrix}, \quad (8)$$

where o τ_{M_i} reactive moment created by the i-th engine;

h – the distance from the center of mass to each of the engines.

Substituting (8) into (9) and expanding the expressions along the axes of the connected coordinate system, we obtain the three differential equations that describe the rotation around the center of mass.

$$\begin{bmatrix}\dot{\omega}_x\\ \dot{\omega}_y\\ \dot{\omega}_z\end{bmatrix}=\begin{bmatrix}\frac{1}{I_x} & 0 & 0\\ 0 & \frac{1}{I_y} & 0\\ 0 & 0 & \frac{1}{I_z}\end{bmatrix}\left[\begin{bmatrix}h(f_4-f_2)\\ \tau_{M_1}-\tau_{M_2}+\tau_{M_3}-\tau_{M_4}\\ h(f_1-f_3)\end{bmatrix}\begin{bmatrix}0 & -\omega_z & \omega_y\\ \omega_z & 0 & -\omega_x\\ -\omega_y & \omega_x & 0\end{bmatrix}\begin{bmatrix}I_x & 0 & 0\\ 0 & I_y & 0\\ 0 & 0 & I_z\end{bmatrix}\begin{bmatrix}\omega_x\\ \omega_y\\ \omega_z\end{bmatrix}\right] \quad (9)$$

The angular position of the quadcopter relative to the earth coordinate system $M_1X_gY_gZ_g$ is set by three angles: ψ - yaw angle, γ - roll angle, ϑ - pitch angle. The relationship between these angles and the angular velocities around the axes of the body-fixed coordinate system is given by the following differential equations:

$$\begin{bmatrix}\dot{\psi}\\ \dot{\gamma}\\ \dot{\vartheta}\end{bmatrix}=\begin{bmatrix}\frac{\omega_y\cos\gamma+\omega_z\sin\gamma}{\cos\vartheta}\\ \omega_x+\tan\vartheta\left(\omega_y\cos\gamma+\omega_z\sin\gamma\right)\\ \omega_y\sin\gamma+\omega_z\cos\gamma\end{bmatrix} \quad (10)$$

The relationship between the connected and the ground coordinate systems is given by a matrix of the direction cosines (11) of the yaw, roll and pitch angles.

$$C_{(\psi,\gamma,\vartheta)}=\begin{pmatrix}\cos\vartheta\sin\psi & \sin\gamma\cos\psi-\cos\gamma\sin\vartheta\sin\psi & \cos\gamma\cos\psi+\sin\vartheta\sin\gamma\sin\psi\\ \cos\vartheta\cos\psi & -\sin\gamma\sin\psi-\cos\gamma\sin\vartheta\cos\psi & -\cos\gamma\sin\psi+\sin\vartheta\sin\gamma\cos\psi\\ \sin\vartheta & \cos\gamma\cos\vartheta & -\sin\gamma\cos\vartheta\end{pmatrix} \quad (11)$$

The spatial displacement of the aircraft is described by the guidance cosine matrix (11) and the linear velocities in the body-fixed coordinate system.

$$\begin{bmatrix} \dot{X} \\ \dot{Y} \\ \dot{Z} \end{bmatrix} = C_{(\psi,\gamma,\vartheta)} \begin{bmatrix} V_z \\ V_y \\ V_z \end{bmatrix}. \tag{12}$$

The system of differential equations describing the movement of the quadcopter consists of the expressions (7, 9, 10, 12). The state vector contains the following variables $(V_x V_y V_z \omega_x \omega_y \omega_z \psi \gamma \vartheta XYZ)$.

Mathematical Model of an Octacopter

The mathematical model of the octacopter is analogous to the model of the quadcopter. The difference between the two models is in the expressions for the external forces and moments acting on the two apparatuses. The external forces acting on the octacopter are described by the following expressions:

$$\begin{bmatrix} F_x \\ F_y \\ F_z \end{bmatrix} = \begin{bmatrix} -G.sin(\vartheta) \\ f_1 + f_2 + f_3 + f_4 + f_5 + f_6 + f_7 + f_8 - G.cos(\gamma)cos(\vartheta) \\ G.sin(\gamma)cos(\vartheta) \end{bmatrix} \tag{13}$$

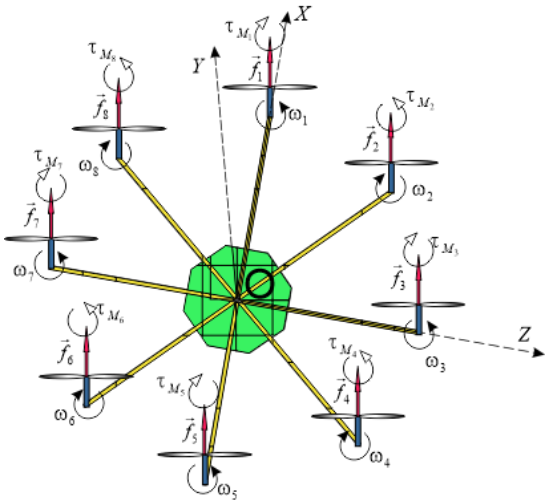

Figure 4. The distribution of external forces and moments acting on a octacopter

The external moments acting on the octacopter are:

$$\begin{bmatrix} M_x \\ M_y \\ M_z \end{bmatrix} = \begin{bmatrix} h(f_7 - f_3) + \text{hcos}\,45^{\circ}(f_8 + f_6 - f_4 - f_2) \\ \tau_{M_1} - \tau_{M_2} + \tau_{M_3} - \tau_{M_4} + \tau_{M_5} - \tau_{M_6} + \tau_{M_7} - \tau_{M_8} \\ h(f_1 - f_5) + h\cos 45^{\circ}(f_2 - f_4 - f_6 + f_8) \end{bmatrix} \tag{14}$$

Substituting (13) into (2) and (14) into (4), we obtain the differential equations for the translational and rotational motion of the aircraft. The mathematical model of the octacopter also includes equations (10) and (12). The state vector is analogous to that of the quadcopter and contains the following variables $(V_x V_y V_z \omega_x \omega_y \omega_z \psi \gamma \vartheta XYZ)$.

Implementation of Mathematical Models in SIMULINK

The simulation of the mathematical models of the quadcopter and the octacopter was performed in the Simulink environment. Each of the two models represents a classical control system with negative feedback and a PID controller (Salih et al.,2010). The initial setting of both regulators was performed according to the second method of Ziegler-Nichols (Copeland, 2008). After receiving working regulators, their coefficients were re-adjusted in order to achieve minimal over-regulation, maximum speed and accuracy. The parallel

implementation in Simulink is shown in Figure 5. The simulations were carried out under the same initial conditions and with the same input signals (desired values of yaw, roll, pitch and flight altitude).

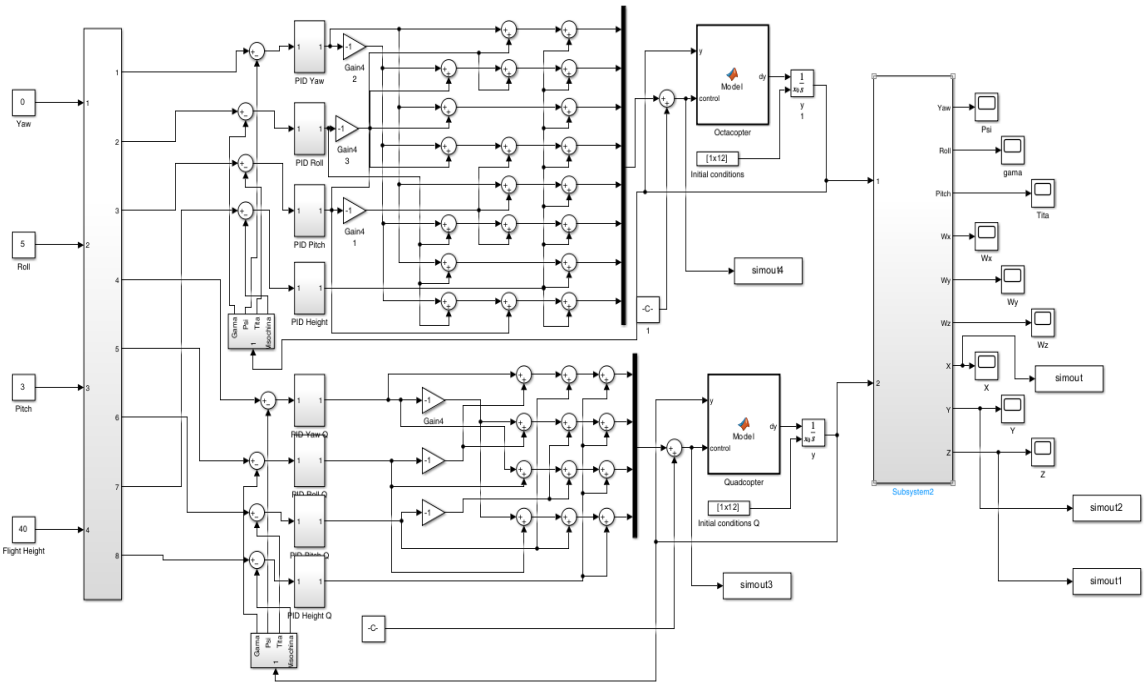

Figure 5. Quadcopter and octacopter model in simulink.

The parallel simulation results are shown in Figures 6 , 7 8 and 9 , where the red graph is the quadcopter response and the blue graph is the octacopter response. The initial conditions of both models are the same$\left(V_x = 0;\ V_y = 0;\ V_z = 0;\ \omega_x = 0;\ \omega_y = 0;\ \omega_z = 0; \psi = 0; \gamma = 0;\ \vartheta = 0;\ X = 0;\ Y = 0;\ Z = 20;\right)$. The initial conditions shown correspond to hovering at a height of 20m. at yaw $\psi = 0^{\circ}$.

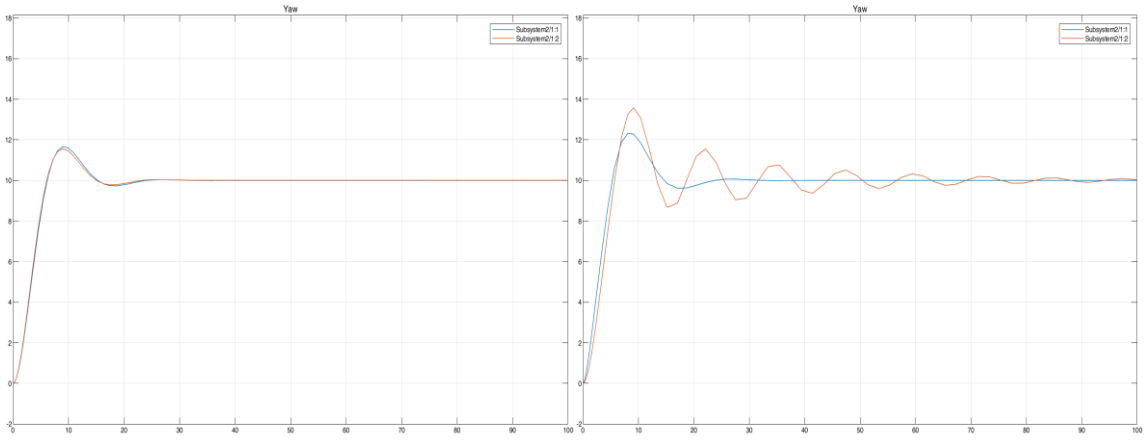

a) b)

Figure 6. Quadcopter

Figure 6a shows the response of the two models when the heading input changes from 0 to 10°. The other inputs (for roll, pitch and height) are equal to zero. Figure 6b shows the course variation of the two models when the input signals change simultaneously, respectively:

- for a yaw from 0 to 10°;
- for roll from 0 to 10°;
- for pitch from 0 to 3°;
- for a height of 20 to 30 m.

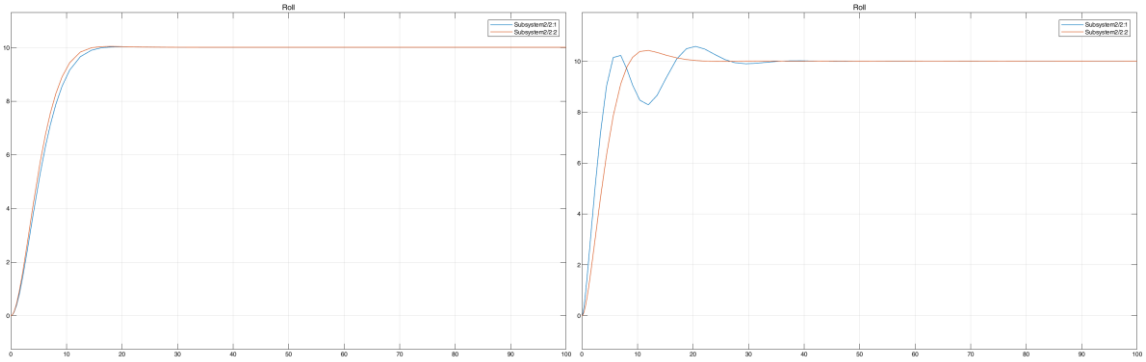

a) b)

Figure 7. Quadcopter

Figure 7a shows the response of the two models when the roll input changes from 0 to 5°. The other inputs (for heading, pitch and altitude) are equal to zero. Figure 7b shows the variation of the roll of the two models when the input signals change simultaneously, respectively:

- for a course from 0 to 10°;
- for roll from 0 to 10°;
- for pitch from 0 to 3°;
- for a height of 20 to 30 m.

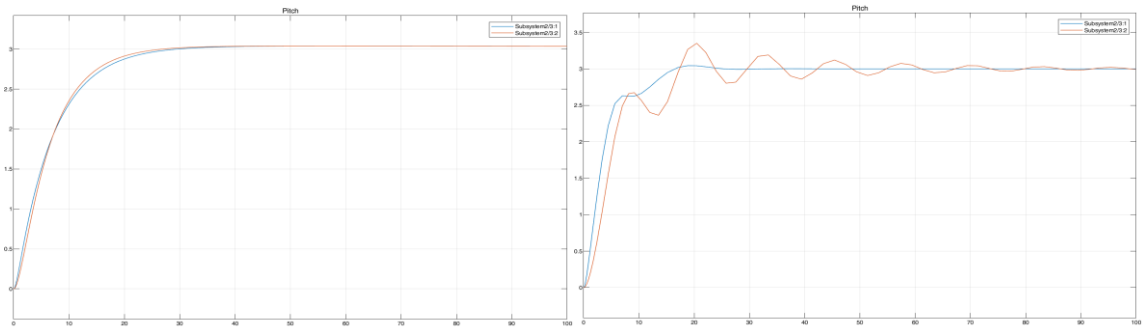

a) b)

Figure 8. Quadcopter

Figure 8a shows the response of both models when the pitch input changes from 0 to 3°. The other inputs (for course, roll and altitude) are equal to zero. Figure 8b shows the change in the pitch of the two models when the input signals change simultaneously, respectively:

- for a course from 0 to 10°;
- for roll from 0 to 10°;
- for pitch from 0 to 3°;
- for a height of 20 to 30 m.

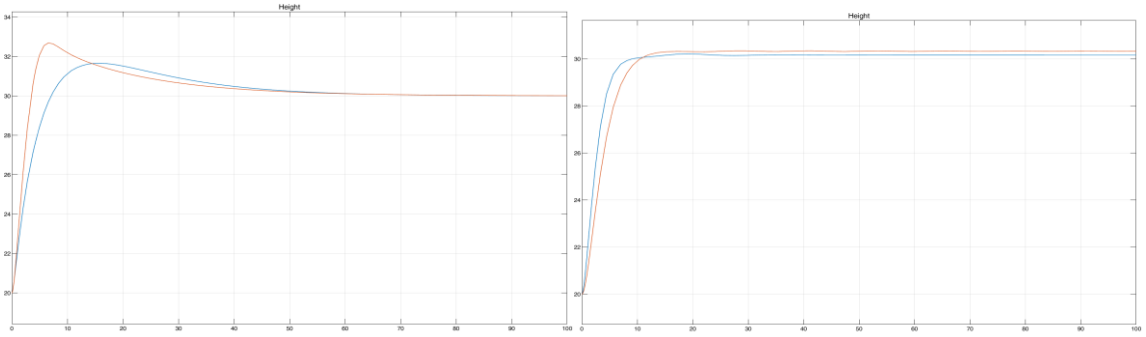

a) b)

Figure 9. Quadcopter

Figure 9a shows the response of the two models when the input signal changes for a height of 20m to 30m. The other inputs (for course, roll and pitch) are equal to zero. Figure 9b shows the change in height of the two models when the input signals change simultaneously, respectively:

- for a course from 0 to 10°;
- for roll from 0 to 10°;
- for pitch from 0 to 3°;
- for a height of 20 to 30 m.

To determine the energy efficiency of the quadcopter and the octacopter, it is necessary to determine the energy consumed by them when performing the same tasks. The created models, shown in Figure 5, allow the revolutions of the engines to be counted at any moment.The engines used in both models are pre-tested. Figure 10 shows the consumption of an engine with propeller when the revolutions vary from 0 to maximum. Figure 11 shows the same data after polynomial smoothing.

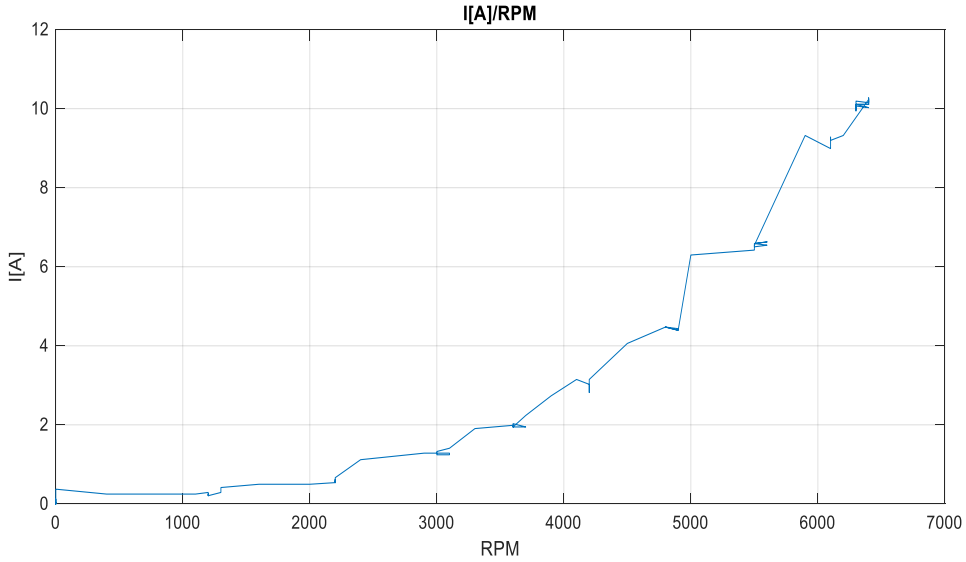

Figure 10. Real data on the consumption of the engines used

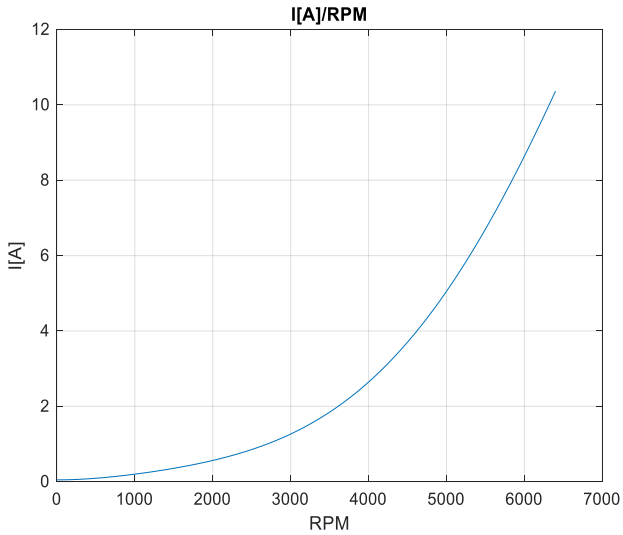

Figure 11. Polynomially smoothed engine consumption data

The duration of the simulation is 100 seconds. The created model allows the revolutions of each engine to be recorded every second, which makes it possible to calculate the energy consumed by them. On average, each of the quadcopter's motors rotated at 5,751 rpm. This means its consumption is 7.6440[A], which for the quadcopter's four motors is 30.5762[A]. On average, each of the octacopter's engines rotated at 4,491 revolutions per minute. Each of its motors consumes 3.6826[A]. The total consumption of the Octacopter is 29.4607[A].

Conclusion

As a result of the simulations and research, the following conclusions can be drawn:
1. Figures 6, 7, 8 and 9 show the faster and more accurate reaching of the desired course, roll, pitch and height values by the octacopter.
2. For the simulation, the octacopter has a lower consumption than the quadcopter. This is due to the higher RPM of the quadcopter motors and the exponential relationship between RPM and energy consumed
3. The results of the present study and those published in Kambushev (2024) show that:
- increasing the number of copter-type drones' engines increases stability and the speed of reaching the desired flight parameters;
- at the same flight weight of the aircraft, those with more engines have a lower energy consumption.

Scientific Ethics Declaration

The authors declare that the scientific ethical and legal responsibility of this article published in EPSTEM Journal belongs to the authors.

Acknowledgements or Notes

* This article was presented as an oral presentation at the International Conference on Advances in Technology and Innovation (www.icati.net) held in Antalya/Turkey on November 14-17, 2024.

*The research in this article was carried out in fulfillment of Task 3.1.9. "Construction of a network of autonomous low-powered aerial devices (quadracopters) for control of an urbanized area" by the National Scientific Program "Security and Defense", adopted by RMS No. 731 of 21.10.2021. and according to Agreement No. D01-74/19.05.2022."

References

Aviastar. (n.d.). *Breguet-Richet gyroplane No.1. helicopter* Retrieved from http://www.aviastar.org/helicopters_eng/breguet_gyro.php

Biliderov, S., Kamenov, K., Calovska, R., & Georgiev, G. (2024). Synthesis and testing of an algorithm for autonomous landing of a UAV under turbulence, wind disturbance and sensor noise. *Engineering Proceedings*, *70*(1), 41.

Copeland, B. R. (2008). *The design of PID controllers using Ziegler Nichols tuning*. Zieglar-Nicholos Method, 1-4.

Georgiev, Y. G. (2022). Battery energy storage technology for aviation – An overview. *Aeronautical Research and Development*, *3*(1), 36-43.

Kambushev, M., (2024). Comparison of flight characteristics of tricopter and quadrocopter. *International Scientific and Technical Conference*, 111-116.

Salih, A., Moghavvemi, M., & Mohamed, H. A. (2010). Flight PID controller design for a UAV quadrotor. *Scientific Research and Essays (SRE)*, *5*(23), 3660-3667.

Author Information

Martin Milenov Kambushev
Georgi Benkovski Bulgarian Air Force Academy
Dolna Mitropolya
5855, 1 Sv. Sveti Kiril I Metodiy St. Bulgaria
Contact e-mail: *m_kambushev@yahoo.com;*

Kiril Milenov Kambushev
Georgi Benkovski Bulgarian Air Force Academy
Dolna Mitropolya
5855, 1 Sv. Sveti Kiril I Metodiy St. Bulgaria

To cite this article:

Kambushev, M.M., & Kambushev, K. M.. (2024). Comparative analysis of the flight characteristics and energy efficiency of a quadcopter and an octacopter. *The Eurasia Proceedings of Science, Technology, Engineering & Mathematics (EPSTEM), 31*, 64-72.